Formation of aerosol at irradiation of targets with laser

T.V. Andrukhova and V.I. Bukaty

Altai State University, Barnaul

Received November 30, 2004

The process of interaction of high-power laser radiation (HPLR) with targets made from aerosol substances is described, as well as the dispersion of the secondary particles affected by the radiation.

By now, a lot of papers have been published on the studies of the influence of laser radiation on solid targets. For example in Refs. 1 to 3 the authors also consider aerosol formation effects. However, one can hardly find any data on the dispersion of the secondary aerosol, which is formed, when substances of solid particles of the atmospheric aerosol are exposed to high-power laser radiation (HPLR). This study aims at experimental investigation of disperse composition and X-ray structure analysis of the aerosol formed under the action of the HPLR on solid samples of some substances.

The flat plate targets were made from $NaHSO_4$, Na_2SO_4, Na_2SO_3, NH_4Cl, PbO, and $FeCl_3 \cdot 6H_2O$. These substances occur in the near-surface atmospheric layer. Cylindrical targets had a diameter about 10 mm and a height ~8 mm. The samples were irradiated by the focused continuous-wave CO_2-laser (the Kipr setup) at a 10.6 μm wavelength and various emission power densities during maximum exposure time of ~8 s.

Under the action of HPLR on a target surface, the substance irradiated was quickly heated, destructed, and then it evaporated. Secondary particles that formed under the laser action were collected on a quartz plate placed at 2 to 5 mm distance from the lens focus. After that, the plate was studied with a microscope and we visually determined the number of particles and took micropictures of them where it was necessary. Besides, we performed an X-ray structure analysis of the above substances by means of the DRON-2 setup. In some cases, the decomposition products were emitted as a luminous plasma jet.

With the increase of the exposure time, we could distinguish three main stages of the substance behavior: I) luminosity of the target, II) appearance and growth of the vapor emission plume, and III) intensive emission of melted particles of different sizes. A lag between the start of laser action and the moment, when vapor first began to appear, was due to the fact that part of the energy in the beginning of irradiation was spent on heating of the target to the temperature, at which there would begin intense vaporization of the substance. This time lag could be estimated by the following expression[3]:

$$\tau \sim T_v^2 \lambda^2 / q^2 a,$$

where T_v is the vaporization temperature; λ is the thermal conductivity; q is the laser flux density (intensity); a is the thermal diffusivity. For example, for a graphite target, at $a = \lambda/(C_p\rho)$ (C_p stands for the specific heat, ρ is the substance density) $\lambda = 40.2$ W/(m · K), $q = 2.14 \cdot 10^9$ W/m^2, $T_v = 3000$–5000 K, $\tau = 1.16 \cdot 10^{-4} - 3.24 \cdot 10^{-4}$ s. In our experiments, the measured time lags and values of T_v are in a good agreement with the above theoretical estimates.

High-rate particle vaporization is characterized by a strong temperature gradient both inside and around the particle (Refs. 4–8). As soon as the vaporized substance is detached from the particle surface, it starts cooling quickly, i.e., an almost adiabatic expansion of a gas–vapor cloud lead to supersaturation of the vaporized matter and is accompanied by condensation of the excess vapor phase.

The condensation process can be divided into two usually non-overlapping stages[4–6]: I) formation of condensation nuclei, II) the condensation itself on the already formed surfaces at a low supersaturation. Target surface temperature essentially depends on interaction regime and has a distinct dynamics.[6–8] In our experiments, we measured temperature using a fast-response optical color pyrometer manufactured at the Department of General Physics of Altai State University and described in Ref. 8. We have measured the surface temperature $T(t)$ of a sample placed in a vacuum cell with ambient pressure p. At the constant values of q and p, the dependence $T(t)$ for different targets did not change qualitatively, but the duration did. With the increase in q and/or decrease in p (within the limits of $10^{-1} - 10^{-2}$ mm Hg), the process duration shortened, and the time of temperature rise to its maximum value shortened as well. The increase in T_{max} value (the highest process temperature) is mainly due to the growth of q, and there is also a weak pressure dependence.

Condensation proceeds until the shock wave (when supersonic dispersal of a substance at a certain distance from a particle abruptly changes for subsonic with the formation of the boundary of an abrupt change of the system's thermodynamic parameters). After that, vapor supersaturation falls down, and substance dispersal is no more accompanied by the exchange between the solid and vapor phases.

0235-6880/05/11 891-05 $02.00

To estimate the laser radiation flux density q, starting from which the substance is intensely evaporated, we can use the relation[3]:

$$q = L\rho(a/\tau_v)^{1/2},$$

where L is the specific evaporation heat; τ_v is the duration of vaporization. When a deep crater has formed on the sample surface, emission of melt becomes considerable. If the sample has a relatively small value of the coefficient a, the emitted melt takes the shape of spherical particles of different sizes that range from 0.4 μm to parts of millimeter.

In such substances as $NaHSO_4$, Na_2SO_4, Na_2SO_3, and NH_4Cl, we could observe boiling of sample surface and appearance of a plasma plume. Besides, after irradiation of PbO, we observed a marked crystallization in the crater with a characteristic metal glance.

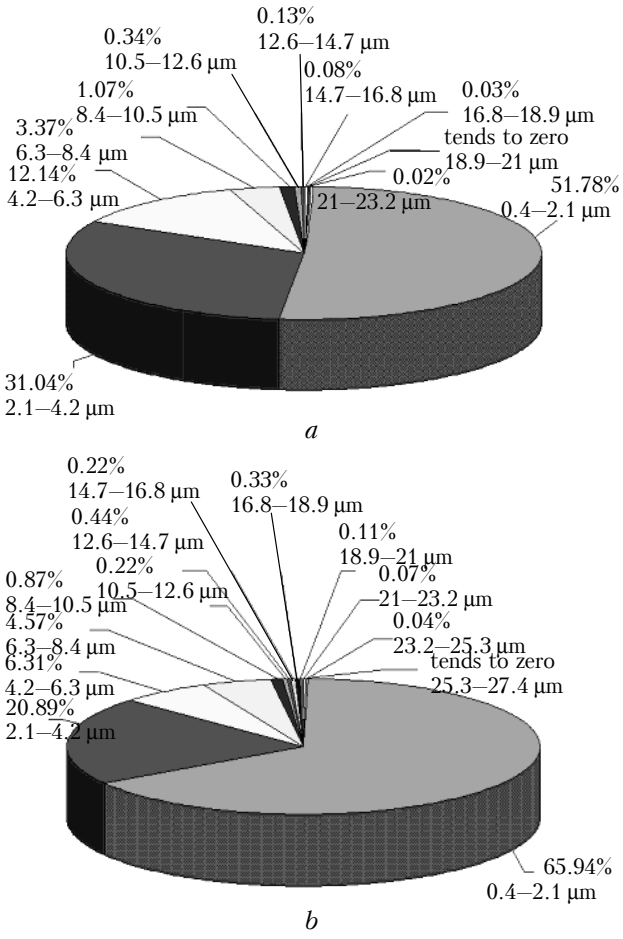

Fig. 1. Percentage distribution of secondary particles of PbO over size at their exposure to HPLR: at a reduced pressure (*a*); under normal conditions (*b*).

Percentage distribution of secondary particles under the action of HPLR on targets and lognormal distribution of some of the above substances are shown in Figs. 1 and 2. More than 90% of the particles formed during vaporization fall within the size of 0.4 to 6 μm. For PbO and Na_2SO_3, at a pressure change, we also noticed a change in percentage of small and large particles in the particle size distribution. The latter fact is illustrated in Fig. 1 for PbO. In all the considered substances, large particles are aggregates of small ones. The most probable reason for this is growth of vaporization rate at pressure reduction and, consequently, decrease in the probability of particle collision at the condensation growth.

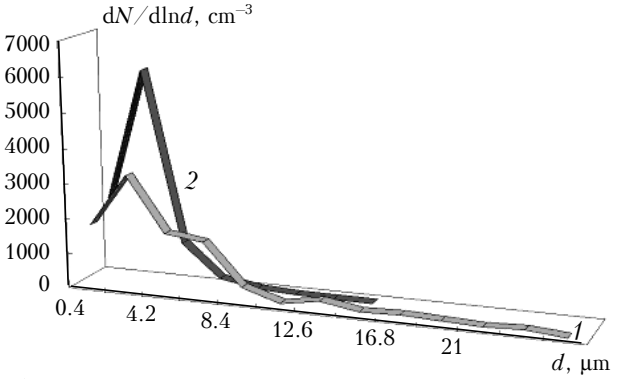

Fig. 2. Size distribution of secondary particles generated at interaction of PbO with HPLR: under normal conditions (*1*); at a reduced pressure (*2*).

Condensation takes place under exposure to laser radiation. We managed to observe formation of long threads of particles, which is generally characteristic of the particles in strong electric fields, where they accrete with other particles. Experimentally, we recorded formation of melt and condensation particles.

We considered the principle of formation of condensation particles theoretically[5,6] and experimentally.[8] It consists in the following: laser radiation heats the target to the boiling point, and the arising vapor jet flow into the environment. Acceleration of vapor to the sonic speed occurs in a thin layer near the surface; here, vapor cools abruptly and transforms to the supersaturated state, which then passes to the saturated state due to abrupt change in condensation. Depending on the environmental conditions (pressure and temperature), a substance can exist in different forms and states.

At relatively low pressures (forevacuum) and temperatures (~ 1000 K), a vaporized substance condenses; the condensate structure can be regular (pure crystals) or irregular (a liquid, amorphous bodies, alloys, polymers). Sometimes, structure properties of a condensed substance can be intermediate compared with those of a solid crystal and a liquid (liquid or mesomorphic crystals). Undergoing a series of structure transformations, the condensed substance finally takes a volume-centered structure.

Thus, in our experiments, we have obtained: fractal clusters composed of small particles; melt drops with their surface crystallized as mono- and polycrystals; elements of fragmented target substance (Fig. 3).

Fractal structures feature self-similarity. Particles can aggregate in three ways[3]: 1) diffusion-confined aggregation; 2) cluster–cluster aggregation; 3) chemically confined aggregation. Each mechanism has its own fractal dimensions. In the first case, the aggregates

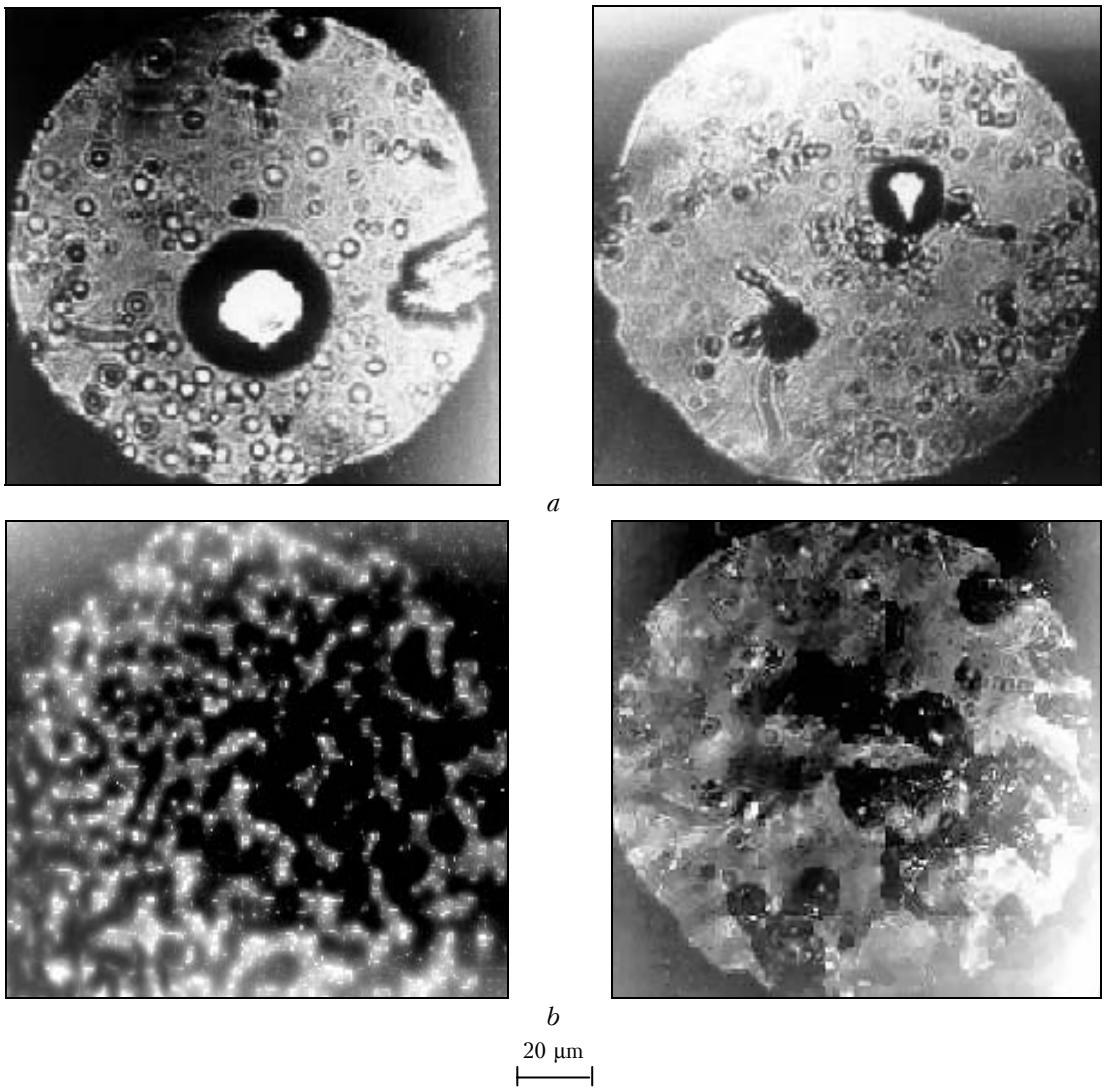

Fig. 3. Photos of secondary particles sedimented on the quartz plate at different distances from the targets made from Na_2HSO_4 (*a*) and NH_4Cl (*b*).

grow by attaching separate randomly moving particles. In the second case, particles first cluster in small aggregates, which then grow, but in this case, large aggregates are loose. The third mechanism is something intermediate between the above two ones and features a large number of interparticle contacts before the particles start aggregating. Under the exposure to laser, most likely is the second mechanism works, which is characterized by the lowest fractal dimensions and loosest aggregates.

Along with the study of the sizes of secondary particles we studied the surface temperature dynamics $T(t)$ of irradiated samples with a fast-response optical color pyrometer with a time resolution of $\sim 10^{-4}$ s (Fig. 4). This pyrometer measures temperature in the range from 1100 to 3000 K. In Fig. 4, the initial part of the process corresponds to temperature at the lower measurement boundary.

Analysis of these experimental dependences $T(t)$ allows us to isolate three temperature intervals in each of the curves. In the first interval, during the time Δt_1 (~ 0.5 s) from the beginning of lasing, the sample is quickly heated up to the maximum temperature T_{max}.

In the second interval, which corresponds to the time Δt_2 (2–8 s), the target is burnt off, while substance temperature in the exposed zone changes insignificantly. It changes abruptly in the third interval, Δt_3 (2–7 s), due to the stop of HPLR action and consequent sample cooling. In all the diagrams, in the third interval, we can see a linear temperature dependence on time. This temperature dependence, $T(t)$, is observed for all samples irregardless of different substances they are made from.

Strongest noise is recorded at the temperature peak of PbO. This phenomenon is caused by the fact that during exposure, under high temperature, there occurs a reaction between lead monoxide and substances in air that yields a gas–vapor cloud of secondary products with their subsequent recondensation and a pure lead in the target crater crystallizing with sample cooling. This was observed both visually and

established in the X-ray structure analysis of the sample (before and after its exposure to laser radiation) and secondary particles. A cooled sample of lead monoxide is characterized by the presence of an air bubble with a layer structure of its walls and its outer surface reminding a cuboctahedron, a truncated octahedron, or a truncated cuboctahedron. An X-ray structure analysis of considered substances showed the following.

The X-ray photograph of ammonium chloride (NH_4Cl) before its exposure to the HPLR is almost the same as the photograph of this substance after its exposure to laser radiation. Positions of diffraction maxima remain unchanged, and the ratio of intensities is almost the same. We suppose that chemical composition of this substance does not undergo any changes at the laser exposure, neither does its original crystal structure.

For ferric chloride ($FeCl_3 \cdot 6H_2O$), positions of diffraction maxima do not change, but there is some change in the ratio of peak intensities. Apparently, chemical composition of the original substance is not affected by laser radiation.

From the analysis of the X-ray photograph, the original lead oxide (PbO) is one of the modifications of this compound (namely, massicot with some incorporations of red lead oxide). After laser action, the resulting substance has the structure of massicot. At the same time, on the photograph, there are a few low-intensity peaks, evidently, caused by the impurities. Because of the low intensity of the diffraction peaks, it was impossible to identify their composition or character.

For sodium sulfate (Na_2SO_4), sodium sulfite (Na_2SO_3), and sodium bisulfate ($NaHSO_4$), the X-ray photographs of the original substances considerably differ from the photographs taken after their exposure to the HPLR. The diffraction peaks corresponding to the original substance are now accompanied by additional maxima, which can be attributed to either the appearance of high-temperature modifications of the substance (for Na_2SO_4) or the products of partial decomposition (for Na_2SO_3 and $NaHSO_4$) in the form of polysulfides of $Na_2S_2O_n$ type and crystallohydrates, which have a large number of crystal structure modifications.

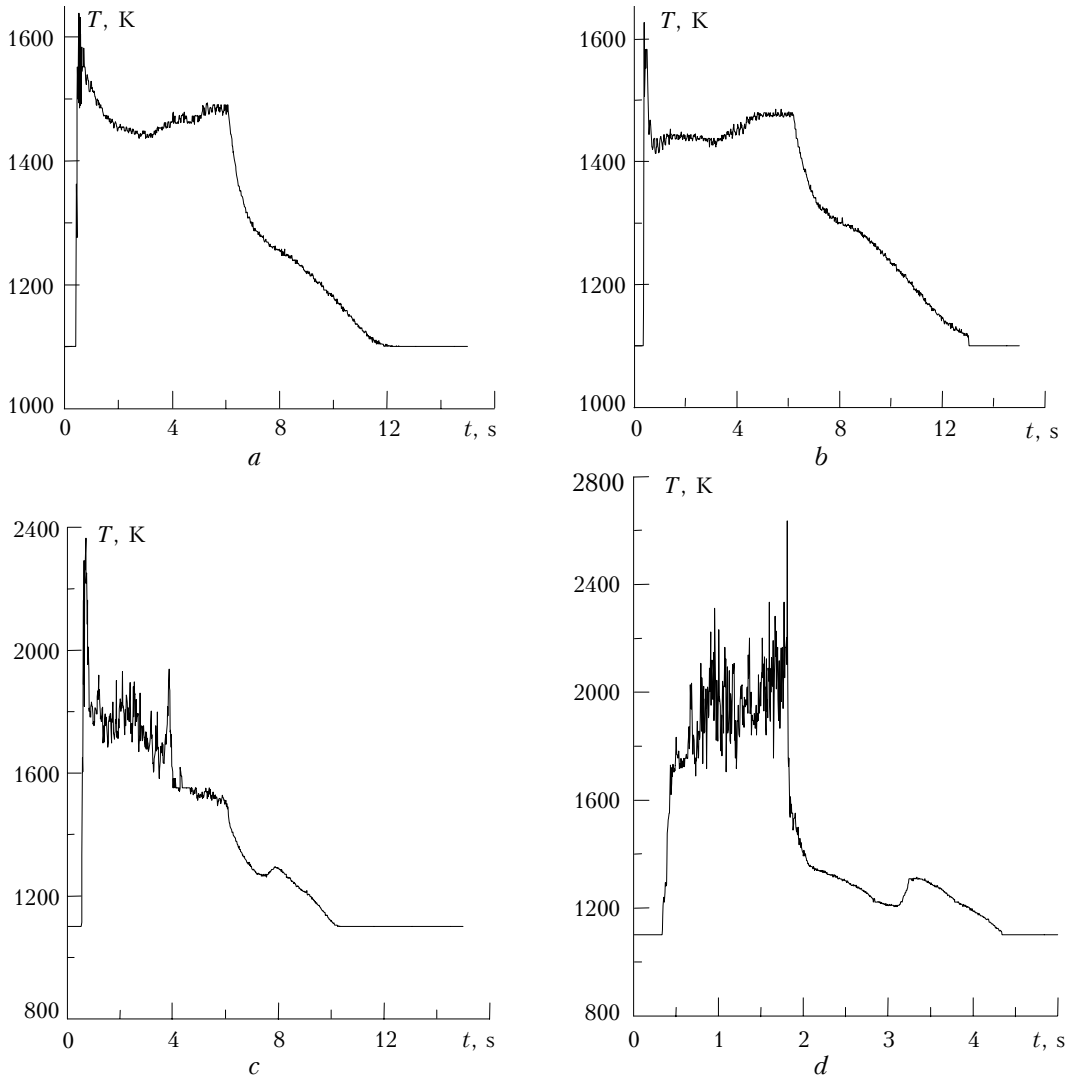

Fig. 4. Temperature dynamics at HPLR action with the intensity $q \sim 10^8$ W/m^2 on the targets made of Na_2SO_3 and PbO: at reduced pressure (*a, c*); at normal conditions (*b, d*).

Thus, after exposure to laser radiation, the resulting substance either has the same chemical composition, maybe, with some modifications in its crystal structure, or becomes a mixture of the original substance and the products of partial decomposition, namely, polysulfides and crystallohydrates.

Finally we would like to note that for most of the substances considered we have observed a change in the ratio of diffraction peak intensities. The cause of this as well as determination of modifications of the resulting chemical substance and the products of partial decomposition need for further analysis.

References

1. Yu.E. Geints, A.A. Zemlyanov, V.E. Zuev, A.M. Kabanov, and V.A. Pogodaev, *Nonlinear Optics of the Atmospheric Aerosol* (Publishing House of SB RAS, Novosibirsk, 1999), 260 pp.
2. V.E. Zuev, Yu.D. Kopytin, and A.V. Kuzikovsky, *Nonlinear Optical Effects in Aerosols* (Nauka, Novosibirsk, 1980), 184 pp.
3. A.V. Pakhomov, *"Aerosols of laser plasma,"* Cand. Phys.-Math. Sci. Dissert., Moscow, 1990, 118 pp.
4. V.I. Bukaty and K.V. Solomatin, in: *Abstracts of Reports at the IV Symp. on Atmospheric and Ocean Optics,* Tomsk (1997), p. 102.
5. V.I. Bukaty and K.V. Solomatin, in: *Abstracts of Reports at the IV Symp. on Atmospheric and Ocean Optics*, Tomsk (1997), p. 101.
6. V.I. Bukaty, G.V. Kuprienko, and K.V. Solomatin, *"Simulation of vaporization processes in a refractory particle and dispersal of evaporated substance in the atmosphere,"* Preprint No. 97/1, Altai State University (1997), 19 pp.
7. L.K. Chistyakova, *"Nonlinear effects at high-power laser pulses propagation in aerosol media. Experiments,"* Doct. Phys.-Math. Sci. Dissert., Tomsk (2001).
8. T.V. Andrukhova, *"Experimental studies of interaction of high-power laser radiation with solid aerosol in vacuum,"* Cand. Phys.-Math. Sci. Dissert., Barnaul, 2001, 198 pp.